TJAA Vol. 7, p.21–29 (2026). DOI: 10.55064/tjaa.1937418 Research Note

Timings of Eclipses in the Light Curves of Selected Post Common Envelope Binaries

Özlem Şimşir[1,2] ⋆, Furkan Akar[1,2], Ezgi Sertkan[1,2], Barış Güler[1,2], Ahmet C. Kutluay[3,1,2], Selçuk Yalçınkaya[4,2], Mohammad Niaei[1,2], İpek Aleyna Ertürk[1,2], Selenay Uçar[4,2], Ekrem M. Esmer[4,2,5], Özgür Baştürk[4,2], Selim O. Selam[4,2]

[1] *Ankara University, Graduate School of Natural & Applied Sciences, Astronomy & Space Sciences Department, Ankara, Türkiye*
[2] *Ankara University, Astronomy and Space Sciences Research and Application Center (Kreiken Observatory), Ankara, Türkiye*
[3] *Astrophysics Group, Keele University, Staffordshire, ST5 5BG, UK*
[4] *Ankara University, Faculty of Science, Astronomy & Space Sciences Department, Ankara, Türkiye*
[5] *Department of Physics and McDonnell Center for the Space Sciences, Washington University, St. Louis, USA*

Accepted: June 4, 2026. Revised: June 4, 2026. Received: April 27, 2026.

Abstract
We present eclipse timings derived from the light curves of selected post-common envelope binaries. Our sample includes systems exhibiting HW Vir-like light curves, pre-cataclysmic variables, and various classes of cataclysmic variables, such as dwarf novae, nova-like variables, and polars.

Key words: binaries: eclipsing – methods: observational – techniques: photometric

1 Introduction

Post-common envelope binaries (PCEBs) are intriguing systems that exhibit eclipse timing variations (ETVs) arising from diverse physical mechanisms. In cataclysmic variables (CVs), the late-type secondary transfers material to the white dwarf primary, resulting in orbital decay due to the changing mass ratio. Conversely, such secular changes are not anticipated in pre-cataclysmic binaries or systems with early-type subdwarf (sdOB) primaries, as their secondaries remain within their Roche lobes. In all these systems, the magnetic activity of late-type secondaries can induce cyclic ETVs via changes in the quadrupole moment, as described by Applegate (1992). Despite many of these secondaries being evolved M-type stars, their magnetic activity may be sustained or regenerated by corotation with the primary in short-period configurations. Furthermore, periodic ETVs in many systems are attributed to the Light-Travel Time Effect (LiTE) caused by substellar companions (Qian et al. 2009, 2010, 2011; Zhu et al. 2015; Wolf et al. 2021; Esmer et al. 2022, 2023b; Baştürk et al. 2023, 2026). These objects, often with minimum masses in the planetary or brown dwarf regimes, may be "first-generation" (forming prior to the common envelope phase) or "second-generation" (forming from the ejected material). While some multi-planetary candidates have been shown to possess unstable orbits (Horner et al. 2011; Hinse et al. 2012; Mustill et al. 2013; Hinse et al. 2014; Song et al. 2019; Esmer et al. 2021, 2023a), there are no fundamental astrophysical barriers to their formation as first-generation objects even with potential changes in their orbital and physical properties (the hybrid scenario), or second-generation objects (Columba et al. 2023; Ledda et al. 2023). Consequently, these systems, for which we provide new eclipse timings, remain a subject of significant interest. Identification of the origin of ETV signals in PCEBs requires long-term timing observations with complementary capabilities. Space-based missions provide high-precision, continuous photometry (Esmer et al. 2024; Esmer & Daylan 2025), while ground-based facilities enable flexible, sustained coverage over longer timescales (Pulley et al. 2025; Yates et al. 2026). In this context, systematic ground-based timing efforts, such as the present study, extend the temporal baseline and enable robust ETV characterization. In addition, the shared evolutionary history and constrained properties of PCEBs make homogeneous catalogs (Sertkan et al. 2025) essential for consistent comparison across systems and for interpreting their underlying physical origins.

In this study, we present 301 new eclipse minima timings (221 primary and 80 secondary) for 58 PCEB systems, including HW Vir-like binaries, pre-cataclysmic variables, and cataclysmic variables. The dataset spans approximately 3 years with typical uncertainties of ∼2-12 seconds. Table 1 summarizes the observations, listing systems, observing dates, minima times, uncertainties, filters, and minima types.

2 Observations and Data Reduction

Some of the observations presented in this study were carried out with the 80 cm, T80 Prof. Dr. Berahitdin Albayrak Telescope at the Ankara University Kreiken Observatory (AUKR) (N 39°50′37″, E $02^h11^m07^s$, at an altitude of 1250 m), while others have been observed with the 1 meter telescope TUG100 at TUG (TÜBİTAK National Observatory, Antalya) at an altitude of 2500 m (N 36°49′27″, E $02^h01^m20^s$).

Observations were performed at one of the Nasmyth foci

⋆ E-mail: ozsmsr@gmail.com

of the T80 telescope at AUKR using a thermoelectrically cooled, back-illuminated Apogee Alta U47+ CCD camera. This detector features a 1024×1024 pixel array with a pixel size of 13 μm. A focal reducer was employed to provide a field of view of 11.84×11.84′. While most data were obtained using the SDSS filter set, a small subset of observations was conducted without a filter (clear) to accommodate the faintness of certain targets. This approach was adopted to achieve a higher signal-to-noise ratio (SNR) and thereby improve the precision of the derived minima timings.

TUG100 telescope at TUG features a 1.0 m primary mirror with an f/10 focal ratio. It is equipped with a cryo-cooled SI 1100 back-illuminated CCD camera, which has a 4096×4096 pixels array and 15 μm pixels, yielding an effective field of view of 21×21 arcmin in the unbinned mode. As the detector readout time is approximately 45 s, a 2×2 binning mode was applied to reduce this to approximately 15 s in most of the observations. This allowed for a higher cadence in the resulting light curves, thereby improving the precision of the minima timings. While most observations used the SDSS filter set, Bessel filters were employed in some cases to achieve a better SNR, as these filters feature transmission curves spanning broader wavelength intervals. A few observations were performed in clear-light mode, such as those of NN Ser, which has a V magnitude of 16.51 and short-lived eclipses.

Target systems were selected using the ObserPy scheduling software (Güler et al. 2025), based on observability during planned runs and constraints such as altitude and lunar proximity during eclipse minima. Exposure times and passbands were chosen according to the brightness of each system and the expected timescales of the eclipse profiles. Data reduction was performed using the `AstroImageJ` (AIJ) software package (Collins et al. 2017); all images were corrected for bias, dark current, and twilight flats to remove systematic effects. We performed differential aperture photometry using AIJ, utilizing 'synthetic' comparison stars composed of ensemble of stars selected for their appropriate brightness, color, and invariability across the observed timescales and wavelengths. The resulting light curves were detrended for linear trends associated with airmass effects that remained after the ensemble differential photometry. Finally, all observation timestamps were converted to BJD-TDB using AIJ.

Representative light curves for NN Ser, DE CVn, V470 Cam, DQ Her, and V1828 Aql are presented in Fig. 1. These examples illustrate the data quality achieved across the different classes of PCEBs included in our sample.

3 Results

Minima times have been derived using the Xtrema software (Bahar et al. 2015) based on the Kwee & van Woerden (1956) method (KvW), which we list in Table 1 and show a few examples with dashed vertical lines in light curve figures (Fig. 1), where dark shade of gray for primary and a lighter shade of gray for secondary minima were used to denote their timings).

It is a well-established principle that the KvW technique (Kwee & van Woerden 1956) is most effective when applied to symmetric minima profiles in the light curves of eclipsing binaries (Deeg 2020). While a significant portion of the timings presented in Table 1 are derived from the V-shaped, symmetric light curves, characteristic of PCEB systems with similar-sized sdOB and dM components (e.g., Fig. 1, right panel), our sample also includes Cataclysmic Variables (CVs) exhibiting total eclipses and asymmetric profiles (e.g., Fig. 1, left panel).

Several alternative methodologies have been proposed as more suitable for such complex light curves, including specialized modeling (Wood et al. 1985; Thoroughgood et al. 2004; Pilarčík et al. 2012) and the application of low-order polynomials Bahar et al. (2015). Furthermore, shifting model light curves to match observations (Esmer et al. 2022) or employing cross-correlation techniques can be attempted, which have been shown to yield higher precision than the KvW method (Esmer et al. 2021). However, the majority of the systems listed in Table 1 possess extensive observational baselines spanning several decades. Because historical timings in the literature have predominantly been determined using the KvW technique, we have opted to maintain this approach to ensure a homogeneous dataset, which is essential for future eclipse timing variation (ETV) analyses. The reliability of this pipeline and the high quality of the resulting measurements have been demonstrated in our recent analysis of the PCEB system DD CrB (Baştürk et al. 2026).

Furthermore, it is recognized that the uncertainties derived via the KvW technique are formal and often underestimated (Mikulášek et al. 2014); the uncertainties presented in Table 1 are no exception. To maintain transparency, we are prepared to provide all primary light curves upon request. We acknowledge that alternative measurement techniques or the derivation of uncertainties through robust methods, such as Monte Carlo sampling, could further refine these values. We reported the results of our timing measurements and their associated formal uncertainties to six decimal places (10^{-6} d) to reflect the numerical precision of the Kwee-van Woerden algorithm and to prevent the loss of information for our highest-quality light curves, even though the physical accuracy for many systems is conservatively estimated at $\sim$2 seconds.

Acknowledgment

We gratefully acknowledge the support by the Scientific and Technological Research Council of Turkey (TÜBİTAK) with the project 122F358.

The data in this study were obtained with the T80 telescope at the Ankara University Astronomy and Space Sciences Research and Application Center (Kreiken Observatory) with various project numbers starting with 23C.T80.06.

We gratefully acknowledge the support by the TUG (TÜBİTAK National Observatory, Antalya) site of the Türkiye National Observatories for the observations obtained by using TUG100 telescope through the project 25ATUG100-3010.

References

Applegate J. H., 1992, ApJ, 385, 621

Bahar E., Şenavcı H. V., Baştürk Ö., 2015, in Rucinski S. M., Torres G., Zejda M., eds, Astronomical Society of the Pacific Conference Series Vol. 496, Living Together: Planets, Host Stars and Binaries. p. 288

Baştürk Ö., Esmer E. M., Demir E., Selam S. O., 2023, Bulletin de la Societe Royale des Sciences de Liege, 92, 11197

Baştürk Ö., et al., 2026, MNRAS, 547, stag290

Collins K. A., Kielkopf J. F., Stassun K. G., Hessman F. V., 2017, AJ, 153, 77

Columba G., Danielski C., Dorozsmai A., Toonen S., Lopez Puertas M., 2023, A&A, 675, A156

Deeg H. J., 2020, Galaxies, 9, 1

Esmer E. M., Daylan T., 2025, AJ, 170, 322
Esmer E. M., Baştürk Ö., Hinse T. C., Selam S. O., Correia A. C. M., 2021, A&A, 648, A85
Esmer E. M., Baştürk Ö., Selam S. O., Aliş S., 2022, MNRAS, 511, 5207
Esmer E. M., Baştürk Ö., Selam S. O., 2023a, Turkish Journal of Astronomy and Astrophysics, 4, 102
Esmer E. M., Baştürk Ö., Selam S. O., 2023b, MNRAS, 525, 6050
Esmer E. M., Baştürk Ö., Selam S. O., Akar F., Sertkan E., Güler B., Yalçınkaya S., 2024, Contributions of the Astronomical Observatory Skalnate Pleso, 54, 228
Güler B., Baştürk Ö., Esmer E. M., Sertkan E., Akar F., 2025, Contributions of the Astronomical Observatory Skalnate Pleso, 55, 466
Hinse T. C., Lee J. W., Goździewski K., Haghighipour N., Lee C.-U., Scullion E. M., 2012, MNRAS, 420, 3609
Hinse T. C., Horner J., Lee J. W., Wittenmyer R. A., Lee C.-U., Park J.-H., Marshall J. P., 2014, A&A, 565, A104
Horner J., Marshall J. P., Wittenmyer R. A., Tinney C. G., 2011, MNRAS, 416, L11
Kwee K. K., van Woerden H., 1956, Bull. Astron. Inst. Netherlands, 12, 327, ADS
Ledda S., Danielski C., Turrini D., 2023, A&A, 675, A184
Mikulášek Z., Chrastina M., Liška J., Zejda M., Janík J., Zhu L.-Y., Qian S.-B., 2014, Contributions of the Astronomical Observatory Skalnate Pleso, 43, 382, ADS
Mustill A. J., Marshall J. P., Villaver E., Veras D., Davis P. J., Horner J., Wittenmyer R. A., 2013, MNRAS, 436, 2515
Pilarčík L., Wolf M., Dubovský P. A., Hornoch K., Kotková L., 2012, A&A, 539, A153
Pulley D., Sharp I. D., Mallett J., von Harrach S., 2025, MNRAS, 544, 24
Qian S.-B., Dai Z.-B., Liao W.-P., Zhu L.-Y., Liu L., Zhao E. G., 2009, ApJ, 706, L96
Qian S.-B., Liao W.-P., Zhu L.-Y., Dai Z.-B., 2010, ApJ, 708, L66
Qian S.-B., et al., 2011, MNRAS, 414, L16
Sertkan E., Baştürk Ö., Esmer E. M., Akar F., Güler B., 2025, Contributions of the Astronomical Observatory Skalnate Pleso, 55, 301
Song S., Mai X., Mutel R. L., Pulley D., Faillace G., Watkins A., 2019, AJ, 157, 184
Thoroughgood T. D., Dhillon V. S., Watson C. A., Buckley D. A. H., Steeghs D., Stevenson M. J., 2004, MNRAS, 353, 1135
Wolf M., Kučáková H., Zasche P., Hornoch K., Kára J., Merc J., Zejda M., 2021, A&A, 647, A65
Wood J. H., Irwin M. J., Pringle J. E., 1985, MNRAS, 214, 475
Yates A., et al., 2026, MNRAS, 547, stag358
Zhu L. Y., Qian S. B., Liao W. P., Fernandez-Lajus E., Soonthornthum B., Zhao E. G., Liu L., 2015, Publication of Korean Astronomical Society, 30, 289

Access:
M26-0103: Turkish J.A&A — Vol.7.

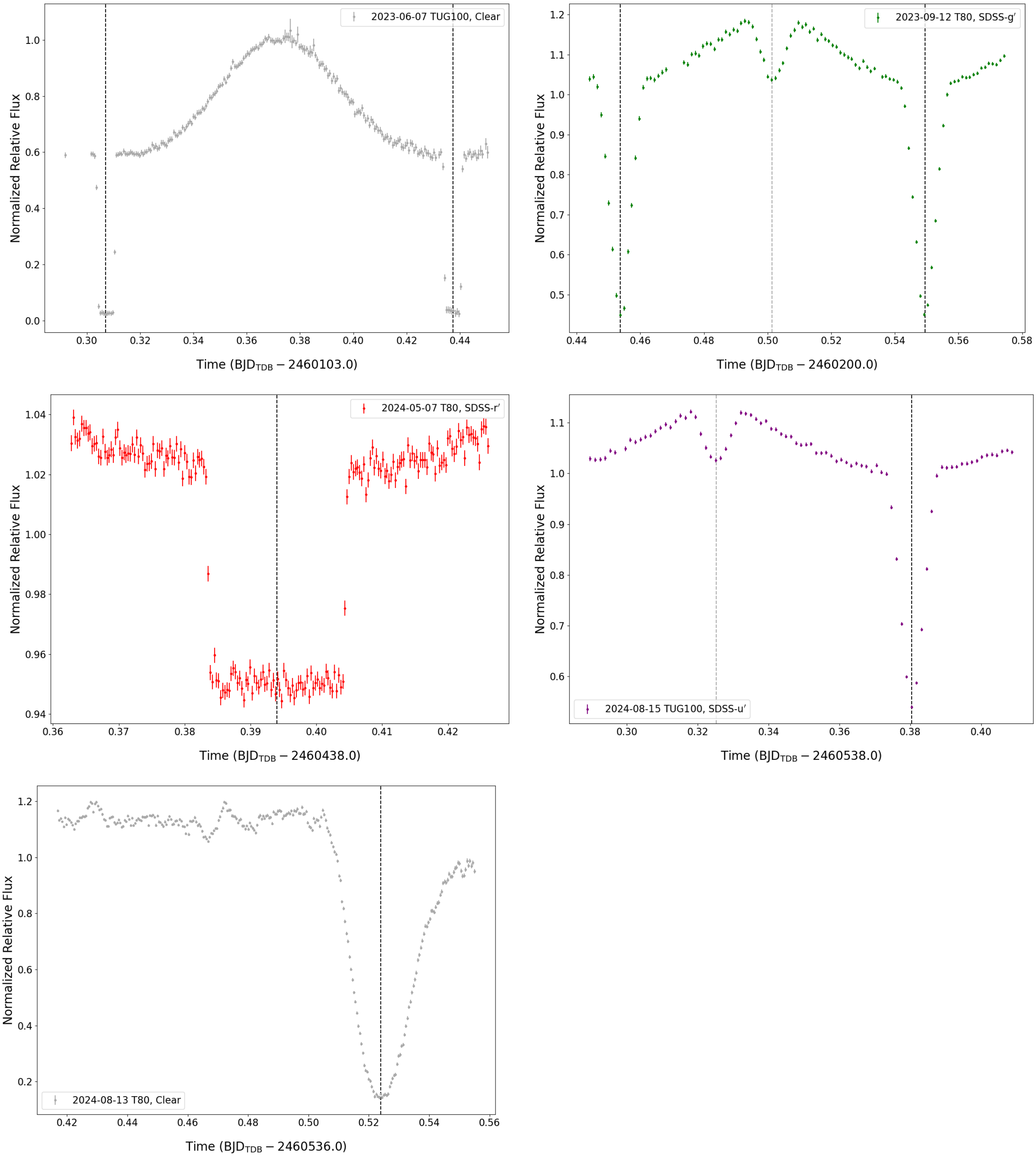

Figure 1. (Top left) Full-phase (clear) light curve of NN Serpentis obtained with TUG100 on 2023-06-07. Vertical dashed lines shows the timings of the eclipse minima. (Top right) Full-phase light curve of V470 Cam (HS 0705+6700) obtained with T80 on 2023-09-12 in SDSS-g′ filter. Vertical dashed lines shows the timings of the eclipse minima. (Mid left) Primary minimum profile of DE CVn obtained with T80 on 2024-05-07 in SDSS-r′ filter. Vertical dashed line shows the timing of the minimum. (Mid right) Full-phase light curve of V1828 Aql obtained with TUG100 on 2024-08-15 in SDSS-u′. Vertical dashed lines shows the timings of the eclipse minima. (Bottom left) Primary minimum profile of DQ Her obtained with T80 on 2024-08-13 without a filter (clear). Vertical dashed line shows the timing of the minimum.

Table 1. The results of minima observations listing UT dates, minima timings in BJD-TDB, associated uncertainties, filters of observations, and the types of the minima (p for primary, s for secondary).

System	UT Date (y-m-d)	$T_{\rm min}$ (BJD-TDB)	Uncertainty (days)	Telescope	Filter	Min. Type
PX And	2023-10-17	2460235.488826	0.000220	TUG100	SDSS-g'	p
	2024-08-12	2460535.511863	0.000129	TUG100	SDSS-r'	p
V1828 Aql	2023-07-01	2460127.347006	0.000018	T80	SDSS-z'	p
	2023-07-01	2460127.402274	0.000062	T80	SDSS-z'	s
	2023-07-06	2460132.424452	0.000082	TUG100	Bessel-B	p
	2023-07-06	2460132.478977	0.000249	TUG100	Bessel-B	s
	2023-07-06	2460132.534747	0.000016	TUG100	Bessel-B	p
	2023-07-29	2460155.326007	0.000060	TUG100	SDSS-u'	s
	2023-07-29	2460155.382243	0.000058	TUG100	SDSS-u'	p
	2023-07-29	2460155.437262	0.000040	TUG100	SDSS-u'	s
	2023-07-29	2460155.492541	0.000035	TUG100	SDSS-u'	p
	2023-08-11	2460168.295933	0.000023	TUG100	Bessel-B	p
	2023-08-11	2460168.351121	0.000033	TUG100	Bessel-B	s
	2024-08-15	2460538.325168	0.000016	TUG100	SDSS-u'	s
	2024-08-15	2460538.380465	0.000005	TUG100	SDSS-u'	p
	2024-08-15	2460538.435498	0.000021	TUG100	SDSS-z'	s
	2024-08-15	2460538.490821	0.000027	TUG100	SDSS-z'	p
UU Aqr	2023-09-10	2460198.438629	0.000059	T80	SDSS-g'	p
	2024-06-16	2460478.488080	0.000024	TUG100	SDSS-g'	p
	2025-07-17	2460874.516223	0.000039	TUG100	Bessel-R	p
HU Aqr	2024-06-15	2460477.513743	0.000487	TUG100	SDSS-r'	p
V363 Aur	2024-10-24	2460608.450374	0.000115	T80	SDSS-r'	p
V470 Cam	2023-08-26	2460183.524320	0.000047	T80	SDSS-g'	p
	2023-08-31	2460188.497647	0.000070	T80	SDSS-g'	p
	2023-09-12	2460200.453751	0.000029	T80	SDSS-g'	p
	2023-09-12	2460200.501769	0.000049	T80	SDSS-g'	s
	2023-09-12	2460200.549431	0.000051	T80	SDSS-g'	p
	2024-02-27	2460368.600697	0.000037	T80	SDSS-g'	p
	2024-03-10	2460380.461174	0.000046	T80	SDSS-r'	p
	2024-03-10	2460380.508656	0.000119	T80	SDSS-r'	s
	2024-03-10	2460380.556677	0.000184	T80	SDSS-r'	p
	2024-04-04	2460405.281590	0.000132	TUG100	SDSS-u'	s
	2024-04-04	2460405.329062	0.000034	TUG100	SDSS-u'	p
	2024-04-04	2460405.376949	0.000063	TUG100	SDSS-u'	s
	2024-04-14	2460415.276324	0.000015	T80	SDSS-z'	p
	2024-04-14	2460415.324233	0.000063	T80	SDSS-z'	s
	2024-05-14	2460445.309397	0.000024	T80	SDSS-r'	p
	2024-05-14	2460445.357194	0.000077	T80	SDSS-r'	s
	2024-05-18	2460449.326308	0.000017	T80	SDSS-r'	p
	2024-05-21	2460452.339424	0.000041	T80	SDSS-r'	s
	2024-05-21	2460452.387301	0.000016	T80	SDSS-r'	p
	2024-10-01	2460585.575279	0.000042	TUG100	Bessel-B	s
	2025-03-21	2460756.448155	0.000037	TUG100	SDSS-z'	p
	2025-03-21	2460756.496296	0.000008	TUG100	SDSS-z'	s
	2025-09-14	2460933.442482	0.000091	T80	SDSS-g'	s
	2025-09-14	2460933.490237	0.000022	T80	SDSS-g'	p
	2025-09-14	2460933.538119	0.000119	T80	SDSS-g'	s
	2025-11-15	2460995.373682	0.000067	T80	SDSS-r'	s
HT Cas	2024-07-14	2460506.463620	0.000014	T80	Clear	p
	2024-07-27	2460519.499005	0.000143	T80	SDSS-r'	p
	2024-10-19	2460603.309607	0.000028	T80	Clear	p
	2024-10-19	2460603.383025	0.000016	T80	Clear	p
	2024-10-19	2460603.456740	0.000013	T80	Clear	p
	2025-09-16	2460935.458377	0.000167	T80	SDSS-g'	p
	2025-09-16	2460935.497922	0.000250	T80	SDSS-g'	s
	2025-10-06	2460955.416911	0.000242	T80	SDSS-g'	p
V1024 Cep	2024-10-15	2460599.455878	0.000065	T80	Clear	p
DE CVn	2023-06-15	2460111.397245	0.000044	T80	SDSS-r'	p
	2024-01-23	2460333.522177	0.000075	TUG100	SDSS-i'	p
	2024-05-07	2460438.394018	0.000034	T80	SDSS-r'	p
DQ Her	2023-06-15	2460111.332514	0.000094	T80	SDSS-r'	p
	2023-10-05	2460223.248020	0.000128	T80	Clear	p

Table 1 – *continued.*

System	UT Date (y-m-d)	T_{min} (BJD-TDB)	Uncertainty (days)	Telescope	Filter	Min. Type
	2023-10-24	2460242.220206	0.000018	T80	SDSS-g'	p
	2024-05-05	2460436.421637	0.000125	T80	SDSS-r'	p
	2024-08-13	2460536.524019	0.000032	T80	Clear	p
	2025-09-09	2460923.379638	0.000300	TUG100	SDSS-g'	p
BH Lyn	2025-03-12	2460747.365867	0.000168	T80	SDSS-g'	p
BP Lyn	2024-10-14	2460598.569953	0.000068	T80	SDSS-r'	p
V477 Lyr	2024-08-20	2460543.396995	0.000039	T80	Clear	p
V870 Lyr	2023-09-26	2460214.278549	0.000046	T80	SDSS-g'	p
	2024-10-13	2460597.261014	0.000013	TUG100	SDSS-g'	p
LX Ser	2024-05-14	2460445.534163	0.000028	T80	SDSS-g'	p
	2025-06-11	2460838.447074	0.000114	T80	SDSS-r'	p
NN Ser	2023-06-07	2460103.307096	0.000080	TUG100	Clear	p
	2023-06-07	2460103.437308	0.000024	TUG100	Clear	p
SW Sex	2024-02-27	2460368.448134	0.000069	T80	SDSS-g'	p
V471 Tau	2024-10-28	2460612.503497	0.000045	T35	Bessel-R	p
RW Tri	2023-08-15	2460172.539982	0.000025	T80	SDSS-g'	p
	2023-09-14	2460202.453015	0.000282	T80	SDSS-g'	p
	2023-09-26	2460214.510936	0.000034	T80	SDSS-r'	p
	2023-10-17	2460235.380469	0.000009	T80	SDSS-g'	p
	2024-08-20	2460543.551148	0.000030	T80	Clear	p
	2024-10-14	2460598.507524	0.000028	T80	SDSS-i'	p
	2025-08-04	2460892.534700	0.000022	T80	SDSS-r'	p
TT Tri	2024-10-15	2460599.286640	0.000024	T80	Clear	p
	2024-10-24	2460608.223438	0.000068	TUG100	Clear	p
	2025-10-11	2460960.388533	0.000156	T80	SDSS-r'	p
UX UMa	2023-07-10	2460136.355353	0.000018	T80	SDSS-g'	p
	2024-01-23	2460333.419945	0.000015	TUG100	SDSS-g'	p
	2025-07-13	2460870.332936	0.000042	T80	SDSS-g'	p
	2026-04-16	2461147.442330	0.000017	T80	SDSS-g'	p
HW Vir	2024-01-23	2460333.569029	0.000004	TUG100	SDSS-g'	p
	2024-04-21	2460422.392532	0.000017	T80	SDSS-r'	p
NY Vir	2024-04-21	2460422.439889	0.000073	T80	SDSS-g'	p
	2025-06-30	2460857.313770	0.000099	T80	SDSS-g'	p
QS Vir	2023-05-15	2460080.426419	0.000043	TUG100	SDSS-i'	p
	2024-05-05	2460436.364635	0.000125	T80	SDSS-r'	p
ATO J016.9284+48.7552	2024-01-23	2460333.320130	0.000030	TUG100	SDSS-g'	p
ATO J129.0542+08.0399	2023-11-23	2460272.585918	0.000034	TUG100	SDSS-g'	p
	2024-02-27	2460368.297303	0.000055	T80	SDSS-g'	p
	2024-02-27	2460368.385980	0.000057	T80	SDSS-g'	p
	2025-03-23	2460758.340659	0.000022	TUG100	SDSS-g'	p
	2025-03-23	2460758.385392	0.000045	TUG100	SDSS-g'	s
	2025-11-17	2460997.530097	0.000161	T80	SDSS-g'	s
	2025-11-17	2460997.574458	0.000079	T80	SDSS-g'	p
	2025-11-17	2460997.618632	0.000414	T80	SDSS-g'	s
ATO J282.4644-13.6762	2024-05-21	2460452.558265	0.000025	T80	SDSS-g'	p
	2024-07-14	2460506.399631	0.000021	T80	SDSS-g'	p
ATO J283.0316+14.7630	2024-07-27	2460519.430067	0.000028	T80	SDSS-g'	p
	2025-06-25	2460852.375810	0.000141	T80	SDSS-r'	s
	2025-06-25	2460852.471256	0.000045	T80	SDSS-r'	p
	2025-07-01	2460858.374141	0.000017	TUG100	SDSS-u'	p
	2025-07-01	2460858.469547	0.000090	TUG100	SDSS-u'	s
ATO J294.7689+11.1822	2023-08-17	2460174.352750	0.000029	T80	SDSS-g'	p
	2024-05-21	2460452.452844	0.000009	T80	SDSS-g'	p
ATO J306.2869+42.7907	2023-07-29	2460155.484567	0.000055	T80	SDSS-g'	p
	2023-10-24	2460242.358896	0.000024	TUG100	SDSS-g'	p
	2024-08-14	2460537.496738	0.000046	TUG100	SDSS-g'	p
	2025-08-18	2460907.515611	0.000096	TUG100	Bessel-V	p
	2025-08-30	2460918.338358	0.000062	TUG100	SDSS-z'	p
	2025-09-10	2460929.453473	0.000080	T80	SDSS-g'	p
	2025-09-12	2460931.503035	0.000302	T80	SDSS-u'	p
	2025-09-13	2460932.234709	0.000436	T80	SDSS-i'	s
	2025-09-13	2460932.380497	0.000192	T80	SDSS-i'	p
	2025-09-13	2460932.526202	0.000286	T80	SDSS-i'	s

Table 1 – *continued.*

System	UT Date (y-m-d)	T_{min} (BJD-TDB)	Uncertainty (days)	Telescope	Filter	Min. Type
	2025-10-20	2460969.234142	0.000075	T80	SDSS-r'	p
	2025-10-20	2460969.381802	0.000308	T80	SDSS-r'	s
	2025-10-27	2460976.254168	0.000112	T80	SDSS-r'	p
ATO J340.2132+54.6308	2023-07-19	2460145.510508	0.000032	T80	SDSS-g'	p
	2023-08-17	2460174.523502	0.000016	T80	SDSS-g'	p
	2023-09-03	2460191.506821	0.000081	TUG100	SDSS-g'	p
	2023-09-08	2460196.460326	0.000013	TUG100	SDSS-r'	p
	2024-09-13	2460567.262077	0.000128	TUG100	SDSS-i'	p
	2024-11-03	2460618.447832	0.000049	T80	SDSS-g'	p
	2025-07-26	2460883.339786	0.000020	TUG100	Bessel-I	p
	2025-07-26	2460883.457997	0.000075	TUG100	Bessel-V	s
	2025-07-26	2460883.458182	0.000068	TUG100	Bessel-I	s
	2025-07-26	2460883.575782	0.000059	TUG100	Bessel-I	p
	2025-08-18	2460906.338150	0.000079	TUG100	Bessel-V	s
	2025-08-18	2460906.455979	0.000063	TUG100	Bessel-V	p
	2025-08-18	2460906.573784	0.000106	TUG100	Bessel-V	s
	2025-08-22	2460910.347819	0.000036	TUG100	Bessel-B	s
	2025-08-22	2460910.347936	0.000085	TUG100	Bessel-V	s
	2025-08-22	2460910.465942	0.000027	TUG100	Bessel-B	p
	2025-08-22	2460910.465964	0.000030	TUG100	Bessel-V	p
	2025-10-18	2460967.312812	0.000140	TUG100	Bessel-B	p
	2025-10-18	2460967.430234	0.000111	TUG100	Bessel-B	s
	2025-10-18	2460967.548719	0.000461	TUG100	Bessel-B	p
CHSS 3072	2023-06-30	2460126.507661	0.000111	T80	SDSS-g'	s
	2023-07-16	2460142.506737	0.000010	T80	SDSS-g'	p
	2023-09-06	2460194.423608	0.000017	T80	SDSS-r'	p
	2023-09-06	2460194.529151	0.000085	T80	SDSS-r'	s
	2023-09-15	2460203.535487	0.000027	T80	SDSS-i'	p
	2024-09-13	2460567.377667	0.000026	TUG100	SDSS-u'	p
	2024-09-13	2460567.589299	0.000068	TUG100	SDSS-u'	p
	2024-09-29	2460583.270431	0.000023	T80	SDSS-i'	p
	2024-10-22	2460606.368190	0.000014	T80	SDSS-g'	p
	2024-10-22	2460606.368257	0.000031	TUG100	SDSS-z'	p
	2024-10-22	2460606.474143	0.000041	TUG100	SDSS-z'	s
	2025-08-04	2460892.440837	0.000034	TUG100	SDSS-g'	p
	2025-08-04	2460892.440837	0.000034	TUG100	SDSS-i'	p
	2025-08-04	2460892.546788	0.000045	TUG100	SDSS-g'	s
	2025-08-04	2460892.546897	0.000028	TUG100	SDSS-i'	s
EVR-CB-002	2023-10-20	2460238.532579	0.000023	T80	SDSS-r'	p
FBS 0747+725	2023-09-24	2460212.472013	0.000082	T80	Clear	p
	2023-10-05	2460223.509417	0.000027	T80	Clear	p
	2023-10-19	2460237.462257	0.000039	TUG100	SDSS-g'	p
	2024-05-15	2460446.339143	0.000007	TUG100	Clear	p
	2024-10-31	2460615.439331	0.000012	TUG100	SDSS-g'	p
	2025-05-18	2460814.320880	0.000036	TUG100	Clear	p
Gaia DR2 1866796475676061056	2023-08-23	2460180.486561	0.000087	T80	SDSS-g'	p
	2023-08-28	2460185.435341	0.000046	T80	SDSS-g'	p
	2024-07-07	2460499.431986	0.000017	TUG100	Clear	p
	2024-09-12	2460566.488456	0.000019	T80	SDSS-g'	p
Gaia DR2 452620071165540006	2023-09-24	2460212.301198	0.000043	TUG100	SDSS-g'	p
GALEX J082053.6+000843	2023-10-17	2460235.574723	0.000026	TUG100	SDSS-g'	p
	2024-10-22	2460606.582691	0.000048	TUG100	SDSS-g'	p
GALEX J183115.7+134519	2024-10-22	2460606.226098	0.000029	T80	Clear	p
	2025-06-05	2460832.454574	0.000024	TUG100	SDSS-g'	p
	2025-06-05	2460832.551020	0.000061	TUG100	SDSS-g'	s
GALEX J194442.8+544942	2023-07-19	2460145.396376	0.000152	T80	SDSS-g'	s
	2023-07-19	2460145.510508	0.000032	T80	SDSS-g'	p
	2023-08-23	2460180.300056	0.000226	T80	SDSS-g'	s
	2023-08-23	2460180.333383	0.000050	T80	SDSS-g'	p
	2023-08-23	2460180.364387	0.000538	T80	SDSS-g'	s
	2023-10-05	2460223.225116	0.000063	TUG100	SDSS-r'	s
	2023-10-05	2460223.257195	0.000040	TUG100	SDSS-r'	p
	2023-10-05	2460223.290199	0.000149	T80	SDSS-i'	s

Table 1 – *continued.*

System	UT Date (y-m-d)	T_{min} (BJD-TDB)	Uncertainty (days)	Telescope	Filter	Min. Type
	2023-10-05	2460223.321262	0.000084	T80	SDSS-i'	p
	2024-06-15	2460477.343001	0.000059	TUG100	SDSS-r'	p
	2024-06-15	2460477.406936	0.000040	TUG100	SDSS-r'	p
	2024-07-14	2460499.338457	0.000055	T80	Clear	p
	2024-10-08	2460592.381927	0.000036	T80	Clear	p
	2025-05-18	2460814.511475	0.000175	TUG100	SDSS-u'	p
	2025-05-18	2460814.543572	0.000464	TUG100	SDSS-u'	s
	2025-07-07	2460864.461242	0.000385	T80	SDSS-g'	s
	2025-07-07	2460864.493634	0.000022	T80	SDSS-g'	p
	2025-07-17	2460874.342644	0.000152	T80	SDSS-g'	s
	2025-07-17	2460874.374379	0.000098	T80	SDSS-g'	p
	2025-10-13	2460962.276791	0.000049	TUG100	SDSS-g'	p
	2025-10-13	2460962.308419	0.000328	TUG100	SDSS-g'	s
	2025-10-13	2460962.340806	0.000097	TUG100	SDSS-g'	p
	2025-10-13	2460962.372830	0.000051	TUG100	SDSS-g'	s
	2026-03-12	2461112.544468	0.000156	T80	SDSS-g'	p
	2026-03-12	2461112.576470	0.000568	T80	SDSS-g'	s
HE 0516-2311	2023-11-23	2460272.413198	0.000026	TUG100	SDSS-g'	p
	2023-11-23	2460272.504255	0.000075	TUG100	SDSS-g'	p
HS 2231+2441	2023-06-27	2460123.437688	0.000080	T80	SDSS-g'	p
	2023-06-27	2460123.492816	0.000140	T80	SDSS-g'	s
	2023-08-11	2460168.391525	0.000090	TUG100	SDSS-r'	s
	2023-08-11	2460168.446878	0.000020	TUG100	SDSS-r'	p
	2023-08-11	2460168.502286	0.000067	TUG100	SDSS-r'	s
	2023-08-11	2460168.557477	0.000021	TUG100	SDSS-r'	p
	2023-09-16	2460204.277256	0.000036	T80	SDSS-g'	p
	2023-09-16	2460204.332111	0.000137	T80	SDSS-g'	s
	2023-09-16	2460204.443096	0.000122	T80	SDSS-r'	s
	2023-09-16	2460204.498508	0.000065	T80	SDSS-r'	p
	2023-09-16	2460204.554793	0.000139	T80	SDSS-i'	s
	2023-10-05	2460223.408961	0.000127	T80	SDSS-i'	p
	2023-10-05	2460223.464070	0.000182	T80	SDSS-i'	s
	2023-10-19	2460237.232456	0.000040	TUG100	SDSS-u'	p
	2023-10-19	2460237.287503	0.000450	TUG100	SDSS-u'	s
	2024-09-12	2460566.341895	0.000013	T80	SDSS-r'	p
	2024-09-12	2460566.452873	0.000010	T80	SDSS-r'	p
	2024-10-01	2460585.251093	0.000029	TUG100	SDSS-u'	p
	2024-10-01	2460585.307274	0.000098	TUG100	SDSS-u'	s
	2024-10-01	2460585.363189	0.000057	TUG100	SDSS-z'	p
	2024-10-01	2460585.417812	0.000089	TUG100	SDSS-z'	s
	2024-10-28	2460612.346317	0.000057	TUG100	SDSS-z'	p
	2024-10-28	2460612.402636	0.000080	TUG100	SDSS-z'	s
	2025-07-08	2460865.482207	0.000034	T80	SDSS-r'	p
	2025-07-17	2460874.438416	0.000153	T80	SDSS-z'	p
	2025-07-17	2460874.493607	0.000363	T80	SDSS-z'	s
	2025-08-29	2460917.347779	0.000028	TUG100	SDSS-u'	p
	2025-08-29	2460917.403410	0.000077	TUG100	SDSS-u'	s
	2025-08-29	2460917.458728	0.000055	TUG100	SDSS-z'	p
	2025-08-29	2460917.514251	0.000064	TUG100	SDSS-z'	s
Kepler-451	2024-10-15	2460599.372128	0.000041	T80	SDSS-g'	p
	2025-10-06	2460955.287740	0.000067	T80	SDSS-r'	p
	2025-10-06	2460955.350882	0.000116	T80	SDSS-r'	s
KPD 2045+5136	2023-11-04	2460253.243824	0.000015	TUG100	SDSS-g'	p
	2024-04-21	2460422.489217	0.000021	T80	SDSS-g'	p
	2024-06-16	2460478.337110	0.000030	TUG100	SDSS-g'	p
	2024-08-12	2460535.349665	0.000033	TUG100	SDSS-r'	p
	2024-08-13	2460536.335794	0.000041	T80	Clear	p
	2025-06-30	2460857.436138	0.000231	T80	SDSS-g'	p
	2025-06-30	2460857.526023	0.000329	T80	SDSS-g'	p
	2025-08-01	2460889.528263	0.000029	TUG100	SDSS-g'	p
	2025-08-11	2460899.299062	0.000228	T80	SDSS-i'	p
	2025-08-24	2460912.479979	0.000046	TUG100	SDSS-i'	p
	2025-08-31	2460919.289682	0.000033	TUG100	SDSS-z'	p

Table 1 – *continued.*

System	UT Date (y-m-d)	T_{min} (BJD-TDB)	Uncertainty (days)	Telescope	Filter	Min. Type
	2025-08-31	2460919.335525	0.000099	TUG100	SDSS-z'	s
	2025-08-31	2460919.378957	0.000023	TUG100	SDSS-u'	p
	2025-08-31	2460919.423250	0.000081	TUG100	SDSS-u'	s
	2025-08-31	2460919.468977	0.000024	TUG100	SDSS-g'	p
	2025-08-31	2460919.513639	0.000067	TUG100	SDSS-g'	s
	2025-09-30	2460949.320325	0.000028	T80	SDSS-g'	p
LAMOST J071857.66+073913.2	2023-10-19	2460237.520812	0.000029	TUG100	SDSS-g'	s
	2023-10-19	2460237.562923	0.000014	TUG100	SDSS-g'	p
	2023-10-19	2460237.605188	0.000035	TUG100	SDSS-g'	s
	2024-10-15	2460599.563864	0.000019	TUG100	SDSS-g'	p
	2024-11-12	2460627.433638	0.000010	TUG100	SDSS-g'	p
	2024-11-12	2460627.476320	0.000043	TUG100	SDSS-g'	s
	2024-11-12	2460627.518064	0.000011	TUG100	SDSS-g'	p
	2024-11-28	2460643.441509	0.000033	TUG100	SDSS-g'	s
	2025-03-23	2460758.266568	0.000008	TUG100	SDSS-g'	p
PG 1628+181	2023-07-16	2460142.360324	0.000035	T80	SDSS-g'	p
	2024-08-14	2460537.336659	0.000042	TUG100	SDSS-g'	p
PN A66 46	2023-09-05	2460193.373802	0.000090	TUG100	SDSS-g'	p
	2023-09-14	2460202.336512	0.000142	T80	SDSS-r'	p
TIC 13111800	2023-07-10	2460136.437151	0.000069	T80	SDSS-i'	p
	2024-05-30	2460461.514971	0.000030	TUG100	SDSS-g'	p
	2024-10-15	2460599.364079	0.000071	TUG100	SDSS-g'	p
	2024-10-22	2460606.450949	0.000109	T80	SDSS-g'	p
	2025-09-14	2460933.357053	0.000224	T80	SDSS-r'	p
TIC 240872692	2024-10-22	2460606.291854	0.000055	T80	Clear	p
TIC 322390461	2024-05-07	2460438.485379	0.000014	T80	Clear	p
	2024-10-01	2460585.506081	0.000023	TUG100	Clear	p
TIC 380964844	2024-10-15	2460599.451654	0.000052	TUG100	Clear	p
TIC 408187719	2024-10-15	2460599.538353	0.000100	T80	Clear	p
TIC 45206965	2024-03-24	2460394.275548	0.000111	T80	SDSS-g'	p
TIC 459182998	2023-08-28	2460185.531084	0.000087	TUG100	SDSS-g'	p
TIC 609725827	2024-10-13	2460597.536389	0.000030	TUG100	Clear	s
	2024-10-13	2460597.590410	0.000020	TUG100	Clear	p
Ton 301	2023-10-21	2460239.542420	0.000091	TUG100	SDSS-i'	p
	2023-10-24	2460242.499747	0.000011	TUG100	SDSS-g'	p
	2024-10-31	2460615.548843	0.000046	TUG100	SDSS-i'	p
	2025-11-15	2460995.439315	0.000926	T80	SDSS-r'	s
	2025-11-15	2460995.439712	0.000455	T80	SDSS-g'	s
	2025-11-15	2460995.623973	0.000034	T80	SDSS-r'	p
	2025-11-15	2460995.624009	0.000062	T80	SDSS-g'	p
	2026-03-12	2461112.271314	0.000667	T80	SDSS-g'	s
	2026-03-12	2461112.272841	0.000523	T80	SDSS-r'	s
	2026-03-12	2461112.456181	0.000069	T80	SDSS-r'	p
	2026-03-12	2461112.456310	0.000109	T80	SDSS-g'	p
UCAC2 23234937	2023-09-10	2460198.298516	0.000010	T80	SDSS-g'	p
UCAC4 489-038954	2025-11-17	2460997.460831	0.000039	T80	SDSS-g'	p
	2025-11-17	2460997.503124	0.000081	T80	SDSS-g'	s
ZTF J192014.13+272218.1	2023-08-23	2460180.426220	0.000036	T80	SDSS-g'	p
	2023-10-21	2460239.277013	0.000035	TUG100	SDSS-g'	p
	2024-10-28	2460612.247071	0.000124	TUG100	SDSS-g'	p